ACADEMIC PRESS

Available online at www.sciencedirect.com
SCIENCE DIRECT®

Journal of Catalysis 213 (2003) 281–290

JOURNAL OF CATALYSIS

www.elsevier.com/locate/jcat

Chromium(III) supported on aluminum-nitride-surfaced alumina: characteristics and dehydrogenation activity

R.L. Puurunen,* S.M.K. Airaksinen, and A.O.I. Krause

Helsinki University of Technology, Laboratory of Industrial Chemistry, PO Box 6100, FIN-02015 HUT, Finland

Received 2 July 2002; revised 29 August 2002; accepted 19 September 2002

Abstract

Chromium catalysts were prepared by the saturating chemisorption of chromium(III) acetylacetonate ($Cr(acac)_3$) at 200 °C on alumina and on alumina that had been surfaced with aluminum nitride. According to elemental analysis, infrared spectroscopy, and electron spin resonance spectroscopy, chemisorption occurred through ligand exchange reaction of $Cr(acac)_3$ with surface OH and NH_x groups and dissociation of $Cr(acac)_3$ or Hacac on coordinatively unsaturated sites on the surface. Steric hindrance imposed by the acac ligands defined saturation of the surface with adsorbed species; the same chromium loading (0.64 ± 0.06 atoms per nm^2) was obtained on all supports. After removal of the ligands with oxygen, water, or ammonia, the samples were active in isobutane dehydrogenation. For chromium sites with high activity, nearby oxygen ions were needed. The activity of a Cr^{3+} ion was mainly determined by its environment and not by whether it had been formed through reduction.

Keywords: Chromium catalyst; Aluminum nitride; Chromium(III) acetylacetonate; Atomic layer deposition; ALD; Alkane dehydrogenation

1. Introduction

Nitrides are interesting candidates for catalyst supports: they are known as hard and thermally stable materials, and their use offers a different type of metal–support interaction from that on more conventional oxide supports [1–9]. Nitrides in bulk form or prepared through nitridation of the surfaces of porous oxide materials have been successfully tested as catalyst supports in dehydrogenation [1–3], hydrogenation [4], dehydrocyclization [5], vinylation [6], oxidation [7], ammonia synthesis [8], and isomerization [9]. However, the number of publications dealing with the use of nitrides as catalyst supports is limited, partly because of the difficulty of producing nitrides in porous high-surface-area forms suitable for catalytic application.

Atomic layer deposition (ALD) is a technique suitable for preparing thin layers of nitrides on high-surface-area materials [10–12]. It is based on repeating the separate, saturating reactions of at least two gaseous reactants with the surface of a solid support; build-up of thin films occurs through the reaction of the second reactant with the chemisorbed species left behind by the first reactant. Aluminum nitride has been prepared through repeating the reaction cycles of trimethylaluminum (TMA) and ammonia with silica and alumina supports [13–16]. The content of aluminum nitride on the surface increases in one reaction cycle on average 2.4 AlN units per square nanometer, while the high surface area of the support is retained [14,16]. In addition to nitride species, the aluminum–nitride-surfaced materials contain amino groups (NH_x, $x = 2, 1$), which serve as potential anchoring sites in catalyst preparation [16]. The objective of this work was to investigate the suitability of aluminum-nitride-surfaced alumina, prepared by ALD, as a support for chromium-based dehydrogenation catalysts.

The dehydrogenation activity of supported chromia catalysts is most often attributed to coordinatively unsaturated (c.u.s.) Cr^{3+} ions [17–26]. The types of Cr^{3+} sites that are most active are under debate, however. On the one hand, mononuclear redox Cr^{3+} has been proposed to be the active site (redox Cr^{3+} referring to Cr^{3+} formed through reduction of chromium in higher oxidation states) [19,21,22]. On the other hand, nonredox Cr^{3+} or clustered Cr^{3+} has been concluded to be more active than redox Cr^{3+} or isolated Cr^{3+} [20,25,26]. On the basis of changes in the physicochemical properties, chromia/alumina catalysts can be divided

* Corresponding author.
E-mail address: riikka.puurunen@hut.fi (R.L. Puurunen).

0021-9517/02/$ – see front matter
PII: S0021-9517(02)00016-7

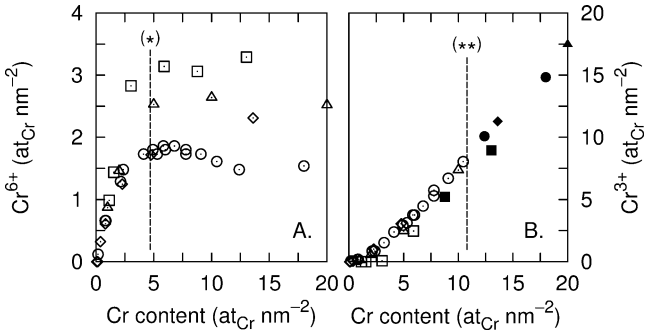

Fig. 1. Summary of the amounts of (A) Cr^{6+} and (B) Cr^{3+} present on oxidized chromia/alumina catalysts as a function of chromium loading (atoms per square nanometer of support), as reported in literature. Note that the y axes in (A) and (B) differ is scale. Cavani et al. [20], squares, De Rossi et al. [21], diamonds, Hakuli et al. [23], circles, and Grzybowska et al. [27], triangles. Full symbols in (B) indicate the presence of XRD-visible α-Cr_2O_3. Lines marked with (∗) and (∗∗) indicate the surface density of chromium on CrO_3 [27] and Cr_2O_3 [29], respectively.

into three main categories with respect to their chromium loading: low-loading catalysts with chromium contents up to about 5 $at_{Cr}\,nm^{-2}$ (chromium atoms per square nanometer), medium-loading catalysts with about 5–11 $at_{Cr}\,nm^{-2}$, and high-loading catalysts with 11 $at_{Cr}\,nm^{-2}$ or more. As summarized in Fig. 1, after calcination with air, low-loading catalysts contain—in addition to Cr^{3+} and some Cr^{5+}—Cr^{6+} whose amount increases with increasing chromium loading [20,21,23,27], whereas on medium-loading and high-loading catalysts the Cr^{6+} content has stabilized to a constant level of about 2–3 $at_{Cr}\,nm^{-2}$ [20,21,23,27]. Cr_2O_3 crystals detectable by X-ray diffraction are typically present only on high-loading catalysts [20–23,27,28]. The changes from one loading category to another coincide with the surface density of chromium on Cr(VI) and Cr(III) oxide: on CrO_3 it is about 5 $at_{Cr}\,nm^{-2}$ [27] and on Cr_2O_3 about 11 $at_{Cr}\,nm^{-2}$ [29]. The catalytic activity of chromia catalysts increases with increasing chromium content for low- and medium-loading catalysts [19,20,23,24,30], but it decreases for high-loading catalysts [20,23,24]. Evidently, for medium- and high-loading catalysts, redox Cr^{3+} sites alone cannot account for the catalytic activity [23,24].

In addition to Cr^{3+}, it has been suggested that nearby oxygen ions participate in the reaction [18,19,31,32]. Dehydrogenation may involve a step where the alkane dissociates to a pair of chromium and oxygen ions to give an alkyl group bonded to surface chromium and a hydrogen bonded to a surface oxygen, schematized as

$$\text{▒Cr–O▒} + \text{R–H} \rightarrow \text{▒Cr–R} + \text{▒O–H}. \quad (1)$$

In the equation, the symbol ▒ denotes the surface. Increased basicity of the oxygen or replacement of the oxygen by more basic nitrogen species could increase the probability of dissociation of the alkane and thus increase the reaction rate [1,2]. Therefore, the use of nitride supports containing basic nitrogen species [33–35] would seem warranted.

Chemisorption of chromium(III) acetylacetonate ($Cr(acac)_3$) was chosen as a method for depositing chromium species on aluminum-nitride-surfaced alumina supports. Saturating chemisorption of $Cr(acac)_3$ at 200 °C on alumina and calcination thereafter with air produces low-loading chromia/alumina catalysts that are active and selective in alkane dehydrogenation [23,30]. Because of the sensitivity of the aluminum-nitride-surfaced supports to oxidation and hydrolysis [16,36–38], the ligands remaining in the $Cr(acac)_3$-modified samples were removed with ammonia instead of the more commonly applied oxygen. The use of ammonia is expected to produce chromium nitride species, in which chromium is in the oxidation state Cr^{3+}, and therefore only nonredox Cr^{3+} should be present during dehydrogenation. Ligand removal with air, in turn, results mostly in redox Cr^{3+} sites [23,24]. Varying the ligand removal agent allowed us to clarify whether redox Cr^{3+} sites alone or also nonredox Cr^{3+} sites are active on low-loading chromium catalysts.

2. Experimental

2.1. Preparation of catalysts

AKZO 001–1.5E alumina, crushed and sieved to a particle size of 250–500 μm, was used as support. Alumina was treated in a muffle furnace and subsequently in vacuum to produce a known number of OH groups. The exact treatment temperatures and times are given in Table 1. The unmodified alumina supports will be referred to in the form "800 °C alumina," where the temperature indicates the heat treatment temperature. The surface areas of the 200, 400, 560, and 800 °C alumina samples were 255, 255, 255, and 196 $m^2\,g^{-1}$ and the OH group contents were 8.7, 6.0, 2.0, and 1.2 OH nm^{-2}, respectively [15].

The catalysts were prepared in an atomic layer deposition (ALD) reactor (ASM Microchemistry, Finland) operating in a vacuum of about 1–5 kPa. There was a continuous flow of nitrogen of about 200 $cm^3\,min^{-1}$ through the reactor. The aluminum nitride modification consisted of repeating the reactions of TMA and ammonia at 150 and 550 °C on 800 °C alumina. Each reaction was allowed to saturate, and the reactor was purged before introduction of the next precursor to avoid uncontrolled deposition. After the modification, the samples were transferred inertly to a nitrogen-filled glove box. The aluminum-nitride-surfaced supports have been characterized in detail earlier [16]. In this work, samples with two and six reaction cycles of TMA and ammonia were used, and they are referred to as $2{\cdot}AlN/Al_2O_3$ and $6{\cdot}AlN/Al_2O_3$ (together as $n{\cdot}AlN/Al_2O_3$). The $2{\cdot}AlN/Al_2O_3$ and $6{\cdot}AlN/Al_2O_3$ samples had surface areas of 193 and 167 $m^2\,g^{-1}$ and hydrogen atom contents in NH_x groups of 3.8 and 7.2 $at_H\,nm^{-2}$, respectively [16]. For the $Cr(acac)_3$ modification, the $n{\cdot}AlN/Al_2O_3$ samples were transferred back to the ALD reactor.

Table 1
Results of elemental analysis for the $Cr(acac)_3$-modified samples

Support	Pretreatment (°C/h)		Cr (wt.%)		C (wt.%)		C/Cr ratio	
	In air	In vacuum	Top	Bottom	Top	Bottom	Top	Bottom
$2{\cdot}AlN/Al_2O_3$	–	550/6[a]	0.9[b]		3.1[b]		15.1[b]	
$6{\cdot}AlN/Al_2O_3$	–	550/6[a]	0.9[b]		3.2[b]		15.9[b]	
200 °C alumina	–	200/10	1.5	1.3	4.4	4.4	13.0	14.0
400 °C alumina	–	400/10	1.4	1.4	4.8	5.0	14.4	15.7
560 °C alumina	600/16	560/4	1.2	1.2	4.0	4.3	14.2	16.0
800 °C alumina	800/16	560/3	1.0	1.1	3.2	3.6	14.6	14.7
800 °C alumina[c]	800/16	560/3	0.9	1.0	3.1	3.3	14.7	14.9

[a] Pretreatment for 4 and 2 h in ammonia and nitrogen, respectively.
[b] Average value in bed.
[c] Repeated preparation.

During the transfer the samples inevitably were slightly exposed to air, which removed nitrogen [16,38]. To regenerate the aluminum nitride surface, the samples were treated with ammonia at 550 °C for 4 h and flushed with nitrogen for 2 h before being reacted with $Cr(acac)_3$.

The chemisorption of $Cr(acac)_3$ (Riedel–de Häen, 99%) at 200 °C was investigated on the $n{\cdot}AlN/Al_2O_3$ samples and on 200, 400, 560, and 800 °C alumina. A support bed typically of 5 g was stabilized in the ALD reactor at a reaction temperature of 200 °C. About 2 g of $Cr(acac)_3$ was vaporized under vacuum at 180 °C and directed through the stationary substrate bed. Excess precursor was collected in a condenser tube placed after the reaction space and held at room temperature. After the reaction, the sample bed was purged with nitrogen for 2 h to remove any unreacted $Cr(acac)_3$. Thereafter, either the system was cooled in nitrogen to remove the sample from the ALD reactor with the acac ligands intact, or the ligands were removed with ammonia, water, or oxygen. To minimize the thermal decomposition of the acac ligands, the feed was started at 200 °C, and the temperature was gradually increased to 550 °C. Ammonia was used for the ligand removal from the $n{\cdot}AlN/Al_2O_3$ supports, and the ligand removal with ammonia, water, and oxygen was compared for $Cr(acac)_3$-modified 800 °C alumina. After the processing, the samples were transferred inertly to a nitrogen-filled glove box. The samples after ligand removal will be referred to in the form "Cr/Al_2O_3–NH_3," here indicating that $Cr(acac)_3$ was deposited on alumina and the ligands were removed with ammonia, as summarized in Table 2.

2.2. Characterization of the catalysts

After the saturated chemisorption of $Cr(acac)_3$, the homogeneity of the support bed was investigated by analyzing samples from the top and bottom parts of the bed. For measurement of chromium contents, samples were dissolved in a lithium tetraborate flux, the cooled solid was dissolved in diluted nitric acid, and the chromium contents were measured by flame atomic absorption spectroscopy. The carbon contents of the $Cr(acac)_3$-modified alumina samples were determined with a Ströhlein CS-5500 analyzer by burning at 1350 °C in oxygen. The carbon and nitrogen contents of samples prepared on aluminum-nitride-surfaced alumina were measured with a LECO CHN-600 analyzer by burning at 950 °C in air; samples for this analysis were prepared inertly.

The chemisorbed species in the $Cr(acac)_3$-modified samples were qualitatively characterized by diffuse reflectance infrared Fourier transform spectroscopy (DRIFT). Spectra were measured at room temperature in nitrogen with a Nicolet Impact 400 D diffuse reflectance infrared spectrometer as described earlier [15]. To obtain better spectra in the wavenumber range 1700–900 cm^{-1}, which is partially blocked by the alumina lattice vibrations, samples were diluted with dried potassium bromide.

The bonding of $Cr(acac)_3$ on alumina and removal of the acac ligand by burning with oxygen was investigated

Table 2
Results of elemental analysis after acac removal

Code	Support	Ligand removal agent	Element contents (wt.-%)						Element contents ($at_i\ nm^{-2}$)[a]					
			Cr		N		C		Cr		N		C	
			Top	Bottom	Top	Bottom	Top	Bottom	Top	Bottom	Top	Bottom	Top	Bottom
Cr/Al_2O_3–NH_3	800 °C alumina	NH_3	1.1	1.1	0.4	0.5	0.14	0.17	0.7	0.7	0.9	1.1	0.4	0.4
$Cr/2{\cdot}AlN$–NH_3	$2{\cdot}AlN/Al_2O_3$	NH_3	1.1	1.1	0.8	0.8	0.6	0.5	0.7	0.7	1.8	1.8	1.6	1.3
$Cr/6{\cdot}AlN$–NH_3	$6{\cdot}AlN/Al_2O_3$	NH_3	1.1	1.1	3.1	3.0	0.7	0.7	0.8	0.8	8.0	7.7	2.1	2.1
Cr/Al_2O_3–H_2O	800 °C alumina	H_2O	1.0	1.0	–		0.0	0.0	0.6	0.6	–		0.0	0.0
Cr/Al_2O_3–O_2	800 °C alumina	O_2	1.1	1.0	–		0.03		0.6	0.6	–		0.1	

[a] No correction was made in the calculation for the mass of the surface compounds.

by electron spin resonance spectroscopy (ESR). A separate set of samples, where $Cr(acac)_3$ was chemisorbed at 170, 200, and 270 °C on crushed AKZO 000–1.5E alumina [30,39], were subjected to this investigation. X-band spectra were measured at 25 °C in nitrogen with a Bruker ESP380 spectrometer.

To evaluate whether sintering of the samples had taken place during ligand removal, the specific surface areas of the Cr/Al_2O_3–O_2 and Cr/Al_2O_3–H_2O samples and, for comparison, 800 °C alumina were measured by the single-point BET method with Micromeritics FlowSorb II 2300 equipment after degasification for 1 h at 200 °C.

2.3. Isobutane dehydrogenation activity measurements

After acac ligand removal, the samples described in Table 2 were tested in isobutane dehydrogenation. The activities were measured in a continuous flow reaction system consisting of a fixed-bed microreactor, along with a Fourier transform infrared (FTIR) gas analyzer and a gas chromatograph (GC) for on-line product analysis. The catalyst sample (0.1 g) was loaded into the reactor inertly. However, the sample was in contact with air for about 20–30 s when the reactor was transferred to the reaction system. Each catalyst was studied in three successive dehydrogenation–regeneration cycles. The activities were measured at 580 °C under atmospheric pressure. The catalyst was heated to the reaction temperature under nitrogen flow (Aga, 99.999%). The isobutane feed (Aga, 99.95%) with a weight hourly space velocity (WHSV) of 15 h^{-1} was diluted with nitrogen, the molar ratio of isobutane to nitrogen being 3 : 7. The nitrogen was purified with Oxisorb (Messer Griesheim). The isobutane feed was continued for 15 min. The reaction products were monitored by FTIR for the first 6 min on stream, a GC sample was taken after 10 min, and the FTIR analysis was continued after this. After the dehydrogenation step, the catalyst was regenerated with diluted air (Aga, air 99.5%, N_2 99.999%). The catalyst was oxidized at 580 °C with 2% O_2/N_2 for 2 min, with 5% O_2/N_2 for 2 min, and with 10% O_2/N_2 for 30 min. The regeneration products—carbon oxides and water—were analyzed by FTIR. The amount of coke deposited on the catalyst during dehydrogenation was calculated from the measured amounts of carbon oxides.

The reaction products were analyzed on line with a Gasmet FTIR gas analyzer (Temet Instruments Ltd.) equipped with a Peltier-cooled mercury–cadmium–telluride detector and with an HP 6890 gas chromatograph equipped with an HP PLOT/Al_2O_3 "M" column and a flame ionization detector. The FTIR spectra were recorded in the wavenumber range 4000–850 cm^{-1} with a resolution of 8 cm^{-1} and a scanning rate of 10 scans s^{-1}. The analysis cuvette (9 cm^3) was maintained at constant temperature (180 °C) and pressure (103 kPa). The spectra were measured every 3 s during the first 2 min on stream, every 5 s during the next 2 min, and thereafter every 30 or 60 s. With the FTIR, it was possible to analyze quantitatively methane, ethane, ethene, propane, propene, *n*-butane, isobutane, 1-butene, *cis*-2-butene, *trans*-2-butene, 1,3-butadiene, isobutene, benzene, toluene, carbon monoxide, carbon dioxide, and water. The composition of the product stream was calculated by the classical least-squares multicomponent analysis method using an analysis program (Calcmet, Temet Instruments Ltd.) with calibration spectra for the measured compounds. The method for analyzing light hydrocarbons by FTIR has been described in detail elsewhere [40].

The conversions, selectivities, and yields were calculated on a molar basis. The mass balance of carbon in the reactor system was calculated from the amounts of hydrocarbons measured by FTIR during dehydrogenation and was about 99%. The amount of coke deposited on the catalysts during dehydrogenation was low, and the effect on the mass balance of carbon was less than 1%. Thermal reactions in the system were investigated by replacing the catalyst with silicon carbide but otherwise implementing the dehydrogenation procedure as usual. The activity of the alumina support was also measured.

3. Results

3.1. Preparation of the catalysts

3.1.1. Chemisorption of $Cr(acac)_3$

When the white alumina samples and light yellow $n\cdot AlN/Al_2O_3$ samples were modified with the violet $Cr(acac)_3$, the samples turned green. A uniform color in the support bed was taken as a signal of homogeneity of the samples. Almost no residue was left in the evaporation vessel of $Cr(acac)_3$, indicating well-controlled vaporization. In addition, a violet solid condensed at the outlet tubes of the reactor, indicating that excess $Cr(acac)_3$ was transported through the reactor without decomposition.

The chromium and carbon contents were measured for all samples to investigate the mechanism of reaction of $Cr(acac)_3$ with the supports. The results of elemental analysis are summarized in Table 1. In all cases the chromium contents determined in the top and bottom parts of the support bed were the same within analytical error, indicating that saturation of the surface with adsorbed species had been achieved. The carbon contents were slightly higher in the bottom than the top part of the bed, and, accordingly, the C/Cr (mol/mol) ratios were higher for the bottom than the top part. The C/Cr ratios varied between 13 and 16, the lower values being measured for the top samples of the alumina pretreated at low temperatures.

The average chromium and acac ligand contents calculated per square nanometer of the support are shown in Fig. 2. In the calculation, all the carbon was assumed to be in acac ligands, $C_5O_2H_7^-$, the surface area measured for support was used, and the mass of the chemisorbed species was subtracted. The amount of chromium bound per unit surface area was independent of the type of surface and was 0.64

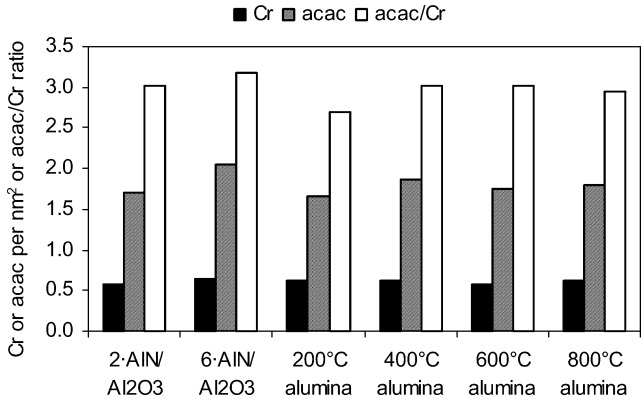

Fig. 2. Average amounts of chromium and acac ligand bound per nm^2 of support and the acac/Cr ratios.

± 0.06 $at_{Cr}\,nm^{-2}$. The average number of ligands left after the chemisorption also did not seem to depend on the type of support and was 1.9 ± 0.2 acac nm^{-2}. With the exception of the 200 °C alumina, the acac/Cr ratio was 3.0 ± 0.1.

DRIFT spectra were measured to investigate the types of surface species generated in the chemisorption of $Cr(acac)_3$ on the alumina and $n{\cdot}AlN/Al_2O_3$ supports. Spectra of the $Cr(acac)_3$-modified samples and of the reference $Cr(acac)_3$ and $Al(acac)_3$ compounds are shown in Fig. 3. Spectra of the $Cr(acac)_3$-modified samples seem almost identical, with some minor differences in the O–H and N–H stretching regions. Comparison with the DRIFT spectra of the supports [15,16] showed loss of the sharp OH bands at about 3791, 3726, and 3690 cm^{-1} and the NH_x bands at about 3395 and 3335 cm^{-1}, indicating that the OH and NH_x groups are involved in the chemisorption of $Cr(acac)_3$. The C–H stretching region (ca. 2800–3100 cm^{-1}) was similar in the sample and reference spectra, indicating that the acac ring structure, at least in part, remains intact in the reaction.

By comparing the DRIFT peaks specific for each metal acac compound in the wavenumber range 1500–1600 cm^{-1}, the acac ligands bonded to chromium and aluminum can be distinguished [41]. The reference spectra measured for $Cr(acac)_3$ and $Al(acac)_3$ and presented in Fig. 3 agree with spectra reported in the literature [41], which possess peaks characteristic of Cr–acac and Al–acac groups, for example at 1575 and 1593 cm^{-1}, respectively. All the sample spectra present peaks similar to those of the reference compounds, indicating in accord with the results for C–H stretching bands that decomposition of acac ligands was insignificant. The presence of two types of acac groups in all samples is revealed by the peaks with maxima at about 1581 and 1598 cm^{-1}. These maxima correspond to Cr–acac and Al–acac groups, respectively. Others have reported a similar shift in the peak positions to higher wavenumbers for supported samples [23,41].

The environment of the chromium was investigated by measuring ESR spectra for $Cr(acac)_3$ and for $Cr(acac)_3$ chemisorbed on alumina. The spectra are presented in Fig. 4. As expected, the spectrum of $Cr(acac)_3$ (curve a) shows one signal: the δ-signal that originates from magnetically isolated Cr^{3+} ions [42]. The δ-signal of isolated Cr^{3+} is also present at about 1000–2000 G in the spectrum of $Cr(acac)_3$-modified alumina (curve b), indicating that most of the chromium ions remained well separated from each other. However, there is also a small β-signal at about 2600–3800 G, which originates from closely packed Cr^{3+} ions in small cluster-like species [42]. Spectra measured for alumina reacted with $Cr(acac)_3$ at different temperatures show that the tendency for cluster formation increases with the reaction temperature. None of the spectra show the γ-signal for Cr^{5+} [42].

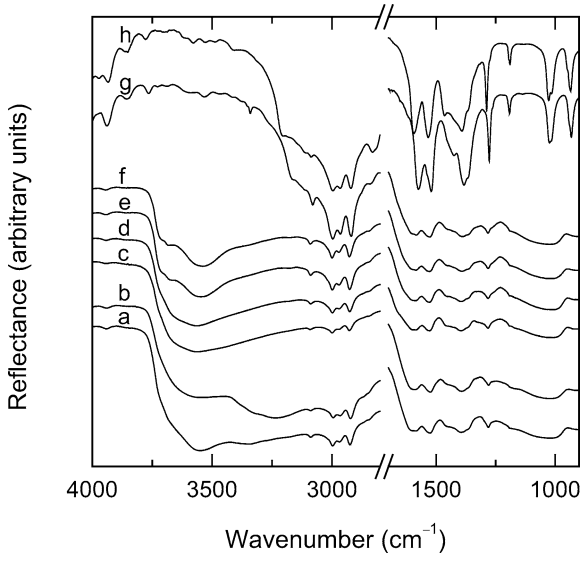

Fig. 3. DRIFT spectra of $Cr(acac)_3$-modified (a) $2{\cdot}AlN/Al_2O_3$, (b) $6{\cdot}AlN/Al_2O_3$, (c) 200 °C alumina, (d) 400 °C alumina, (e) 560 °C alumina, (f) 800 °C alumina, and the reference spectra of (g) $Cr(acac)_3$ and (h) $Al(acac)_3$. Region 4000–2800 cm^{-1} is shown for the spectra of undiluted samples and region 1700–900 cm^{-1} for the KBr-diluted samples.

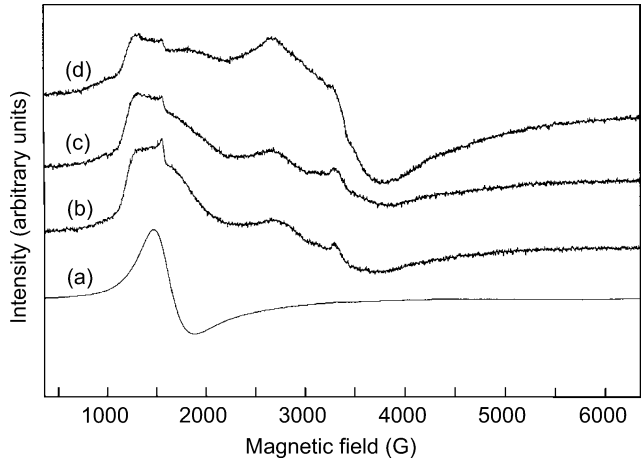

Fig. 4. ESR spectra recorded at 25 °C for (a) $Cr(acac)_3$ and for $Cr(acac)_3$ chemisorbed on alumina (b) at 170 °C (0.7 $at_{Cr}\,nm^{-2}$ and 2.5 acac/Cr), (c) at 200 °C (0.7 $at_{Cr}\,nm^{-2}$ and 2.6 acac/Cr), and (d) at 270 °C (1.0 $at_{Cr}\,nm^{-2}$ and 2.0 acac/Cr). (Spectra have been shifted vertically for clarity.)

3.1.2. Removal of the acac ligands

Ligands were removed from the $Cr(acac)_3$-modified $n\cdot AlN/Al_2O_3$ samples with ammonia and from $Cr(acac)_3$-modified 800 °C alumina with ammonia, water, and oxygen. The results of elemental analysis are summarized in Table 2. Water and oxygen effectively removed the carbon-containing ligands. Ammonia was less effective, with some residual carbon remaining in the samples. The amount of residual carbon in the samples prepared on $n\cdot AlN/Al_2O_3$ supports increased with aluminum nitride content of the support. This was also reflected in the color of the samples: after ligand removal with ammonia, the sample prepared on alumina turned green–gray, whereas the samples prepared on aluminum-nitride-modified alumina turned almost black. DRIFT spectra measured for the samples after ligand removal (not shown) indicated that no acac ligands remained.

The nitrogen contents (Table 2) for the samples prepared on the $2\cdot AlN/Al_2O_3$ and $6\cdot AlN/Al_2O_3$ supports (0.8 and 3.1 wt.%, respectively) are considerably less than the original nitrogen contents of the supports, 1.7 and 5.7 wt.% N, respectively [16]. Some nitrogen was thus lost, and the pretreatment with ammonia did not fully regenerate the surface, in accord with earlier results obtained for AlN/SiO_2 supports [38].

The ESR spectrum measured for the sample after ligand removal with oxygen (not shown) indicated that a shift had taken place, mostly from isolated Cr^{3+} to more clustered Cr^{3+} species. Moreover, part of the chromium species had oxidized to Cr^{5+}. Spectra were not measured for the water-treated and ammonia-treated samples.

The specific surface areas of the 800 °C alumina and the Cr/Al_2O_3–H_2O and Cr/Al_2O_3–O_2 samples, measured by the single-point BET method, were 206, 175, and 199 $m^2\,g^{-1}$, respectively. Therefore, the ligand removal with water had caused somewhat more sintering than the ligand removal with oxygen.

3.2. Dehydrogenation activity

The activities of the catalysts where ligands had been removed (Table 2) were measured in isobutane dehydrogenation. Figure 5 shows the product distribution in the first dehydrogenation step with Cr/Al_2O_3–O_2. The main product obtained with all samples was isobutene. The most significant side reaction was the cracking of C_4 hydrocarbons to C_1–C_3 hydrocarbons. With Cr/Al_2O_3–O_2, the selectivity to isobutene was 91% and to C_1–C_3 hydrocarbons about 8%. In addition, low concentrations (< 1%) of other C_4 hydrocarbons besides isobutane and isobutene was detected. During the first minutes on isobutane stream, samples Cr/Al_2O_3–O_2 and Cr/Al_2O_3–H_2O released reduction products: carbon dioxide, carbon monoxide, and water. This was caused by the reduction of Cr^{5+} and Cr^{6+} with isobutane to Cr^{3+} [18, 22], according to the stoichiometry presented in the equations

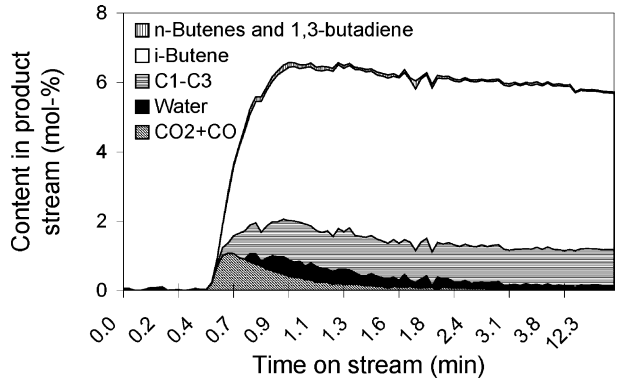

Fig. 5. Product distribution obtained with sample Cr/Al_2O_3–O_2 at 580 °C as measured by FTIR.

$$i\text{-}C_4H_{10} + (4x+5)O^{2-} \rightarrow 4CO_x + 5H_2O + (8x+10)e^-, \quad (2a)$$

$$Cr^{5+} + 2e^- \rightarrow Cr^{3+}, \quad (2b)$$

$$Cr^{6+} + 3e^- \rightarrow Cr^{3+}. \quad (2c)$$

In accord with other investigations [22], the amount of water detected by FTIR during the reduction was lower than anticipated from the stoichiometry of reaction (2a), indicating that some water remained on the catalysts. The amount of reduction products was significantly lower for the Cr/Al_2O_3–H_2O than for the Cr/Al_2O_3–O_2 sample. The samples treated with ammonia did not release any reduction products. After regeneration with diluted air reduction products were released from all samples in the second dehydrogenation step. The amount of reduction products was lower in the third dehydrogenation step than the second, again for all samples. From the product distribution during the first minutes on isobutane stream we estimated the average oxidation state of chromium on the catalysts before dehydrogenation. The values calculated assuming a reduction to Cr^{3+} are shown in Table 3.

Figure 6 shows the yield of isobutene for all samples during the first dehydrogenation step. The Cr/Al_2O_3–NH_3, $Cr/2\cdot AlN$–NH_3, and Cr/Al_2O_3–H_2O samples deactivated slightly faster with time on stream than the $Cr/6\cdot AlN$–NH_3 and Cr/Al_2O_3–O_2 samples. This was not reflected by the coke contents on the catalysts: the Cr/Al_2O_3–O_2 and

Table 3
Average oxidation state of chromium before dehydrogenation[a]

Sample	Average oxidation state of Cr[b]		
	Cycle 1	Cycle 2	Cycle 3
Cr/Al_2O_3–NH_3	3.0	3.8	3.7
$Cr/2\cdot AlN$–NH_3	3.0	4.1	3.8
$Cr/6\cdot AlN$–NH_3	3.0	4.5	4.0
Cr/Al_2O_3–H_2O	3.2	3.8	3.7
Cr/Al_2O_3–O_2	4.9	4.5	4.1

[a] As calculated from the amounts of reduction products released, assuming reduction to Cr^{3+}.

[b] Accuracy of the estimate ±0.1 on average.

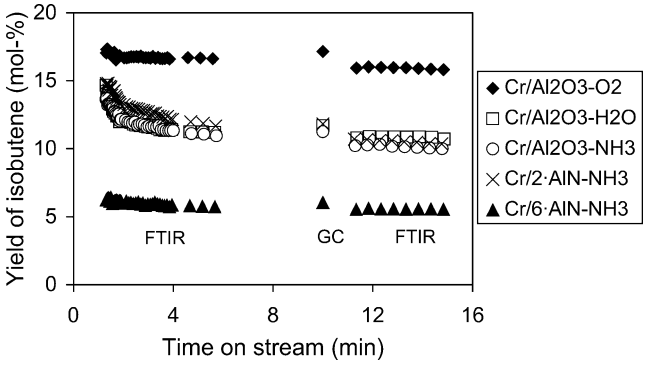

Fig. 6. Yield of isobutene at 580 °C during the first dehydrogenation step.

Cr/Al_2O_3–H_2O samples released 0.30 and 0.14 $mmol_C\ g_{cat}^{-1}$ during the oxidative regeneration after the first dehydrogenation step. Because of residual carbon in the ammonia-treated samples, the amount of coke deposited on them could not be accurately determined. The activities were stable after 10 min, which was chosen as the reference point for further comparison. The choice of reference point did not affect the activity order of the catalysts.

Figure 7 shows the activities of the catalysts after 10 min on isobutane stream in the three successive dehydrogenation steps. The highest yield of isobutene was obtained with the Cr/Al_2O_3–O_2 sample. The Cr/Al_2O_3–NH_3, Cr/2·AlN–NH_3, and Cr/Al_2O_3–H_2O samples exhibited similar activities, and the lowest activity was with the Cr/6·AlN–NH_3 sample. The activity increased in the second dehydrogenation step for the Cr/Al_2O_3–H_2O and Cr/6·AlN–NH_3 samples and decreased for the other samples. The activities decreased for all samples in the third dehydrogenation step.

To investigate the extent of thermal reactions, an experiment was carried out with a reactor filled with inert silicon carbide. This gave an isobutene yield of 2.5%. Alumina calcined at 800 °C gave a similar result. The yield of cracking products—C_1–C_3 hydrocarbons—was not significantly influenced by the presence of a catalyst, indicating that cracking was mainly thermal.

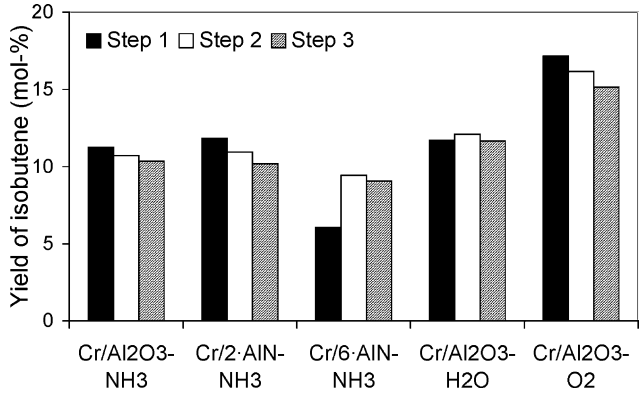

Fig. 7. Yield of isobutene at 580 °C at 10 min on isobutane stream as measured by GC.

The ammonia-treated samples released nitrous oxide (N_2O), in addition to the regeneration products (carbon oxides and water), in the first regeneration step indicating destruction of the nitride structure. Quantitative analysis of the nitrous oxide was unfortunately not possible because of the lack of suitable FTIR calibration spectra. However, the relative amounts of nitrous oxide released were proportional to the nitrogen contents in the samples (Table 2): for Cr/Al_2O_3–NH_3, the nitrous oxide peaks at 2238 and 2215 cm^{-1} were weak and could be seen for about 30 s, for Cr/2·AlN–NH_3 the peaks were more intense and present for about 60 s, and for Cr/6·AlN–NH_3 they were most intense and observable for about 10 min. The FTIR spectra revealed neither ammonia nor other nitrogen oxides besides nitrous oxide during regeneration, nor any nitrogen-containing products during dehydrogenation. Thus, high-molecular-weight nitrogen compounds, whose release has been observed during the dehydrogenation of isobutane on Pt/AlGaPON catalysts [2], were not seen in this study. In the second and third regeneration, the samples released only carbon oxides and water. After the third regeneration, the samples were yellow, indicating the presence of Cr^{6+}.

4. Discussion

4.1. Chemisorption of Cr(acac)$_3$

$Cr(acac)_3$ was chemisorbed at 200 °C on n·AlN/Al_2O_3 samples with different number of NH_x groups and on alumina samples with different number of OH groups. Despite the different bonding sites, the amount of chromium bonded per unit surface area of the support was similar on all supports (see Fig. 2). This trend is unusual for reactants used in ALD: typically, the amount of metal species bonded decreases with decreasing OH group content of the support [11]. Furthermore, in the preparation of cobalt catalysts by the chemisorption of $Co(acac)_3$ on AlN/SiO_2, the amount of cobalt species bonded per unit surface area was found to decrease with increasing aluminum nitride content of the support [38].

The acac/Cr ratio was 3 after the chemisorption of $Cr(acac)_3$ on almost all the supports. Therefore, in addition to the ligand exchange reaction [23,30],

$$\text{▒O–H} + Cr(acac)_3 \rightarrow \text{▒O–}Cr(acac)_2 + Hacac, \quad (3)$$

which alone would result in an acac/Cr ratio of two, other mechanisms must be considered. On alumina, acac/Cr ratios of 3 can form through three types of reactions: (i) dissociative adsorption of $Cr(acac)_3$ on c.u.s. Al–O pairs [23,43,44],

$$\text{▒Al–O▒} + Cr(acac)_3 \rightarrow \text{▒Al–acac} + \text{▒O–}Cr(acac)_2 \quad (4)$$

(ii) associative adsorption [41],

$$\text{▒} + Cr(acac)_3 \rightarrow \text{▒}^{\cdot\cdot}(acac)_2Cr\text{–acac}, \quad (5)$$

and (iii) ligand exchange reaction (3) combined with a secondary reaction of the released Hacac with c.u.s. Al–O sites [44,45] or OH groups of alumina [45]:

$$\text{Al–O} + \text{Hacac} \rightarrow \text{Al–acac} + \text{O–H}, \quad (6)$$

$$\text{Al–OH} + \text{Hacac} \rightarrow \text{Al–acac} + \text{H}_2\text{O}. \quad (7)$$

Similar reactions can probably occur with Al–NH_x sites and c.u.s. Al–N sites on the n·AlN/Al_2O_3 supports. Since DRIFT indicated that Al–acac species had been formed, association (5) seems unlikely to have occurred. The remaining options are dissociative adsorption of $Cr(acac)_3$ on c.u.s. sites (4) and a combination of ligand exchange reaction (3) and readsorption of the released Hacac (6), (7). Since the acac/Cr ratios were systematically slightly higher for the bottom than for the top part of the alumina bed preheated at 200–560 °C, it seems likely that a combination of the ligand exchange reaction and readsorption of Hacac made at least some contribution to the chemisorption of $Cr(acac)_3$. The occurrence of dissociation (4) can neither be verified nor ruled out.

The finding that the acac ligand density on the surface settled at a more or less constant value (1.9 ± 0.2 acac nm^{-2}) in the chemisorption of $Cr(acac)_3$ is of interest. In general, the factor determining the saturation level of chemisorption can be (i) a shortage of suitable bonding sites on the surface or (ii) steric hindrance imposed by the ligands of the chemisorbed species. If there had been a shortage of suitable bonding sites, for example, OH groups on some of the surfaces, the number of bonded chromium species would have decreased with decreasing OH group content of the support. No such trend was seen in this study. A decreasing trend has, in contrast, been observed for the chemisorption of $Cr(acac)_3$ on silica [46–48]. If steric hindrance imposed by the chemisorbed species defined saturation, the ligand density would have remained constant for surfaces with different amounts of bonding sites. The acac ligand density after the $Cr(acac)_3$ chemisorption remained constant, and, furthermore, it was close to the 2.1 ± 0.1 acac nm^{-2} observed for the chemisorption of Hacac at 200 °C on alumina preheated at 300–600 °C [45]. It seems, therefore, that steric hindrance imposed by the ligands, not a shortage of bonding sites on the surface, defines the saturation of the surface with

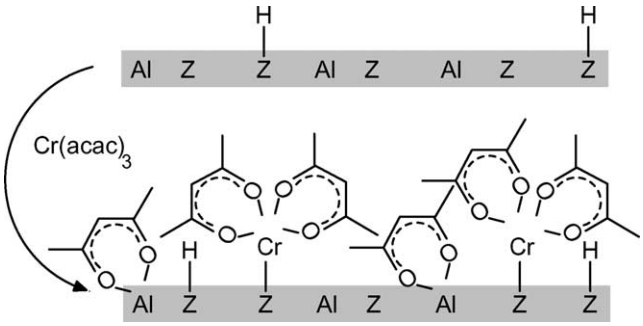

Fig. 8. Schematic representation of the surface species present before and after the chemisorption of $Cr(acac)_3$. Z denotes oxygen or nitrogen.

adsorbed species in the $Cr(acac)_3$ chemisorption on alumina supports [23,30] and on the n·AlN/Al_2O_3 supports. We have summarized the chemisorption of $Cr(acac)_3$ schematically in Fig. 8.

4.2. Active species in dehydrogenation

The samples prepared on n·AlN/Al_2O_3 and on alumina were active in isobutane dehydrogenation after acac ligand removal with ammonia, water, and oxygen. In the first dehydrogenation step, the dehydrogenation activity was significantly lower with the Cr/6·AlN–NH_3 sample than with the other samples (Fig. 7). This could have been due either (i) to the higher content of residual carbon or (ii) to the higher content of nitrogen on the Cr/6·AlN–NH_3 sample. The carbon left on the surface during preparation could have covered some of the chromium sites, thereby blocking them from the isobutane molecules. However, the residual carbon content was almost as high for the Cr/2·AlN–NH_3 sample as for the Cr/6·AlN–NH_3 sample: 1.5 $at_C\,nm^{-2}$ and 2.1 $at_C\,nm^{-2}$, respectively (Table 2). Despite this, the dehydrogenation activity of the Cr/2·AlN–NH_3 sample was similar to the activity of the Cr/Al_2O_3–NH_3 sample, which contained 0.4 $at_C\,nm^{-2}$ carbon. Thus, it seems unlikely that the lower activity was due to the residual carbon alone. Another explanation for the lower dehydrogenation activity may be that a negative ion next to the active Cr^{3+} participates in the reaction [18,19,31,32]. According to low-energy ion scattering, aluminum nitride species cover 30 and 74% of the oxide surface after two and six deposition cycles of TMA and ammonia, respectively, [16]. In the first dehydrogenation step, the probability of finding a nitrogen ion near a chromium ion should thus have been much higher on the Cr/6·AlN–NH_3 sample than on the other samples. Because the activity of this sample was considerably lower, it seems that nitrogen ions are less suitable than oxygen ions for dissociating alkane molecules in dehydrogenation. This result differs from what was anticipated on the basis of the basicity of the nitrogen species [33–35]. The higher activity observed with the Cr/6·AlN–NH_3 sample in the second dehydrogenation step was most likely related to the at least partial oxidation of the nitride phase during regeneration, indicated by the release of nitrous oxide. Our results, therefore, support the idea that the surface oxygen ions play an essential part in the dehydrogenation mechanism on chromium-based catalysts.

The ligand removal agent influenced the dehydrogenation activity: the highest isobutene yield was obtained with the sample prepared on alumina where oxygen was used to remove the acac ligands (Figs. 6 and 7). Activity was lower where water or ammonia was used instead of oxygen, even though the water treatment was effective in removing all the acac ligands. The activity differences can be partly explained by the surface areas of the samples. The surface area was lower with the Cr/Al_2O_3–H_2O sample than with the Cr/Al_2O_3–O_2 sample; ligand removal with water, and

possibly also with ammonia, sintered the support, which most likely caused some of the deposited chromium to become lost from the surface. Thus, a higher number of exposed chromium ions probably contributed to the high activity of the Cr/Al_2O_3–O_2 sample. However, other factors in addition to the surface area may be effective. The high activity of the Cr/Al_2O_3–O_2 sample might have been partially related to its higher redox Cr^{3+} content, as these sites have been suggested to be more active than nonredox sites are [19,21,23]. If this were the case, the activity would increase with the relative amount of redox Cr^{3+} sites. During the first regeneration, part of the chromium was oxidized on all samples (Table 3), but no significant activity increase was observed with the Cr/Al_2O_3–NH_3, $Cr/2{\cdot}AlN$–NH_3, or Cr/Al_2O_3–H_2O samples in the second dehydrogenation step. Thus, higher activity of the redox Cr^{3+} sites compared to the nonredox Cr^{3+} does not explain the high activity observed with the Cr/Al_2O_3–O_2 sample. The high activity could be partly related to the distribution of chromium sites. Two-dimensional clustered Cr^{3+} sites have been suggested to be more active than isolated Cr^{3+} [26,49]. More two-dimensional Cr^{3+} clusters may have formed on the oxygen-treated sample than on the water- or ammonia-treated ones: the Cr/Al_2O_3–O_2 sample contained the highest number of Cr^{6+} ions, which are more mobile than Cr^{3+} and could thus gather in larger groups of chromium ions. ESR indicated the presence of clustered Cr^{3+} (β-phase) after acac ligand removal with oxygen.

During the first dehydrogenation step, the Cr/Al_2O_3–O_2 sample was the only one that contained both redox and nonredox Cr^{3+} sites. Practically no reduction products were released from the other samples (with the exception of small amounts from Cr/Al_2O_3–H_2O). During the second dehydrogenation step this situation changed. After the samples had been regenerated with an oxygen treatment, all samples contained both redox and nonredox Cr^{3+}. Redox Cr^{3+} sites have been proposed to be the only active sites on low chromium-loading catalysts [19,21,23]. If this were the case, the catalysts without redox Cr^{3+} would not have been active. Furthermore, the activity of the catalysts that did not contain redox Cr^{3+} sites in the first dehydrogenation step should have increased notably after the oxidative regeneration. No such increase was observed. Our results suggest that active Cr^{3+} does not need to be formed through reduction of chromium in high oxidation states. Nonredox Cr^{3+} sites can also be active on low-loading chromium catalysts and, furthermore, they are not necessarily less active than redox Cr^{3+} sites.

5. Conclusions

Aluminum-nitride-surfaced alumina was investigated as support for chromium dehydrogenation catalysts. In the preparation of the catalysts by ALD from $Cr(acac)_3$, chemisorption occurred through ligand exchange reaction of $Cr(acac)_3$ with surface OH and NH_x groups, and perhaps through dissociation of $Cr(acac)_3$ on coordinatively unsaturated sites. The Hacac released in the ligand exchange reaction readsorbed on the surface. Steric hindrance imposed by the acac ligands defined the saturation of the surface with adsorbed species. The chemisorption of $Cr(acac)_3$ at 200 °C saturated to a ligand density of 1.9 ± 0.2 acac nm^{-2} and a surface loading of chromium of 0.64 ± 0.06 $at_{Cr}\,nm^{-2}$. Removal of the acac ligands at 550 °C with water and oxygen was complete, whereas removal of the ligands with ammonia left behind some residual carbon. The $Cr(acac)_3$-modified samples from which acac ligands had been removed were active in the dehydrogenation of isobutane. Dehydrogenation activity of the catalysts was lower with the alumina surfaced with aluminum nitride than the alumina support. Evidently, the oxygen ions on the supported chromia catalysts participate in the dissociation of isobutane and their replacement by nitrogen decreases activity. In addition to redox Cr^{3+} sites, nonredox sites were active already at low chromium loadings. Furthermore, redox sites were not more active than nonredox sites.

Acknowledgments

We thank Ms. Mirja Rissanen for the preparation of some samples, Dr. Seppo Kasa (present address Kemira Pigments Oy) for the ESR measurements, and Dr. Arja Hakuli-Pieterse and Dr. Arla Kytökivi for the preparation of the ESR samples. Fortum Oil and Gas Oy, Analytical Research, carried out the chromium, carbon, and nitrogen analyses, and the University of Joensuu, Department of Chemistry, allowed us to use their DRIFT equipment. Funding was received from the Academy of Finland through the Graduate School in Chemical Engineering (GSCE) and the PROTEK program.

References

[1] M.A. Centeno, M. Debois, P. Grange, J. Catal. 192 (2000) 296.
[2] S. Delsarte, F. Maugé, P. Grange, J. Catal. 202 (2001) 1.
[3] D. Hullmann, G. Wendt, U. Šingliar, G. Ziegenbald, Appl. Catal. A 225 (2002) 261.
[4] V.M. Safronov, A.B. Fasman, V.I. Vorob'eva, Izv. Akad. Nauk Kaz. SSR Ser. Khim. 6 (1982) 37.
[5] N. Fripiat, P. Grange, Catal. Lett. 62 (1999) 53.
[6] J. Kiviaho, T. Hanaoka, Y. Kubota, Y. Sugi, J. Mol. Catal. A 101 (1995) 25.
[7] C. Méthivier, J. Massardier, J.C. Bertolini, Appl. Catal. A 182 (1999) 337.
[8] C.J.H. Jacobsen, J. Catal. 200 (2001) 1.
[9] S. Kaskel, K. Schlichte, J. Catal. 201 (2001) 270.
[10] T. Suntola, in: D.T.J. Hurle (Ed.), Handbook of Crystal Growth, Vol. 3, Elsevier, Amsterdam, 1994, pp. 601–663.
[11] S. Haukka, E.-L. Lakomaa, T. Suntola, Stud. Surf. Sci. Catal. 120A (1999) 715.
[12] M. Ritala, M. Leskelä, in: H.S. Nalwa (Ed.), Handbook of Thin Film Materials, Vol. 1, Academic Press, San Diego, CA, 2002, pp. 103–159.

[13] R.L. Puurunen, A. Root, S. Haukka, E.I. Iiskola, M. Lindblad, A.O.I. Krause, J. Phys. Chem. B 104 (2000) 6599.
[14] R.L. Puurunen, A. Root, P. Sarv, S. Haukka, E.I. Iiskola, M. Lindblad, A.O.I. Krause, Appl. Surf. Sci. 165 (2000) 193.
[15] R.L. Puurunen, M. Lindblad, A. Root, A.O.I. Krause, Phys. Chem. Chem. Phys. 3 (2001) 1093.
[16] R.L. Puurunen, A. Root, P. Sarv, M.M. Viitanen, H.H. Brongersma, M. Lindblad, A.O.I. Krause, Chem. Mater. 14 (2002) 720.
[17] F. Buonomo, D. Sanfilippo, F. Trifirò, in: G. Ertl, H. Knözinger, J. Weitkamp (Eds.), Handbook of Heterogeneous Catalysis, Vol. 5, VCH, Weinheim, 1997, pp. 2140–2151.
[18] B.M. Weckhuysen, R.A. Schoonheydt, Catal. Today 51 (1999) 223.
[19] S. De Rossi, G. Ferraris, S. Fremiotti, E. Garrone, G. Ghiotti, M.C. Campa, V. Indovina, J. Catal. 148 (1994) 36.
[20] F. Cavani, M. Koutyrev, F. Trifirò, A. Bartolini, D. Ghisletti, R. Iezzi, A. Santucci, G. Del Piero, J. Catal. 158 (1996) 236.
[21] S. De Rossi, M. Pia Casaletto, G. Ferraris, A. Cimino, G. Minelli, Appl. Catal. A. 167 (1998) 257.
[22] A. Hakuli, A. Kytökivi, A.O.I. Krause, T. Suntola, J. Catal. 161 (1996) 393.
[23] A. Hakuli, A. Kytökivi, A.O.I. Krause, Appl. Catal. A 190 (2000) 219.
[24] A. Hakuli, Doctoral thesis, Helsinki University of Technology, 1999.
[25] S.M.K. Airaksinen, J.M. Kanervo, A.O.I. Krause, Stud. Surf. Sci. Catal. 136 (2001) 153.
[26] R.L. Puurunen, B.M. Weckhuysen, J. Catal. 210 (2002) 418.
[27] B. Grzybowska, J. Słozyński, R. Grabowski, K. Wcicło, A. Kozłowska, J. Stoch, J. Zieliński, J. Catal. 178 (1998) 687.
[28] M. Cherian, M.S. Rao, W.-T. Yang, J.-M. Jehng, A.M. Hirt, G. Deo, Appl. Catal. A 233 (2002) 21.
[29] H.J. Lugo, J.H. Lundsford, J. Catal. 91 (1985) 155.
[30] A. Kytökivi, J.-P. Jacobs, A. Hakuli, J. Meriläinen, H.H. Brongersma, J. Catal. 162 (1996) 190.
[31] R.L. Burwell Jr., A.B. Littlewood, M. Cardew, G. Pass, T.H. Stoddardt, J. Am. Chem. Soc. 82 (1960) 6272.
[32] D.E. Resasco, G.L. Haller, Catalysis 11 (1994) 379.
[33] P. Grange, P. Bastians, R. Conanec, R. Marchand, Y. Laurent, Appl. Catal. A 114 (1994) L191.
[34] S. Delsarte, A. Auroux, P. Grange, Phys. Chem. Chem. Phys. 2 (2000) 2821.
[35] D. Hullman, G. Wendt, G. Ziegenbalg, Chem. Eng. Technol. 24 (2001) 147.
[36] M.A. Centeno, M. Debois, P. Grange, J. Phys. Chem. B 102 (1998) 6835.
[37] M.A. Centeno, P. Grange, J. Phys. Chem. B 103 (1999) 2431.
[38] R.L. Puurunen, T.A. Zeelie, A.O.I. Krause, Catal. Lett. 83 (2002) 27.
[39] A. Kytökivi, Doctoral thesis, Helsinki University of Technology, 1997.
[40] A. Hakuli, A. Kytökivi, E.-L. Lakomaa, O. Krause, Anal. Chem. 67 (1995) 1881.
[41] I.V. Babich, Yu.V. Plyuto, P. Van Der Voort, E.F. Vansant, J. Chem. Soc. Faraday Trans. 93 (1997) 3191.
[42] B.M. Weckhuysen, I.E. Wachs, R.A. Schoonheydt, Chem. Rev. 96 (1996) 3327.
[43] S. Köhler, M. Reiche, C. Frobel, M. Baerns, Stud. Surf. Sci. Catal. 91 (1995) 1009.
[44] J.A.R. van Veen, G. Jonkers, W.H. Hesselink, J. Chem. Soc. Faraday Trans. 85 (1989) 389.
[45] A. Kytökivi, A. Rautiainen, A. Root, J. Chem. Soc. Faraday Trans. 93 (1997) 4079.
[46] S. Haukka, E.-L. Lakomaa, T. Suntola, Appl. Surf. Sci. 75 (1994) 220.
[47] I.V. Babich, Yu.V. Plyuto, P. Van Der Voort, E.F. Vansant, J. Colloid Interface Sci. 189 (1997) 144.
[48] A. Hakuli, A. Kytökivi, Phys. Chem. Chem. Phys. 1 (1999) 1607.
[49] A. Brückner, J. Radnik, D.-L. Hoang, H. Lieske, Catal. Lett. 60 (1999) 183.